

## Hydrogenolysis of glycidol as alternative route to obtain selectively 1,3-propanediol using $\text{MO}_x$ modified Ni-Cu catalysts supported on acid mesoporous saponite

Fiseha B. Gebrestadik<sup>a</sup>, Jordi Llorca<sup>b</sup>, Pilar Salagre,<sup>\*,a</sup> Yolanda Cesteros<sup>a</sup>

Ni and Cu mono- and bi-metallic catalysts modified with various types of acid oxides  $\text{MO}_x$  ( $M = \text{Mo}, \text{V}, \text{W}$  and  $\text{Re}$ ) were tested for hydrogenolysis of glycidol, as alternative route to hydrogenolysis of glycerol to obtain 1,3-propanediol. Characterization results revealed that the presence of modifiers affected dispersion and reducibility of the NiO particles, and the strength and amount of the acid sites. Among the modifiers tested, Re showed the highest activity, high propanediols selectivity and the highest 1,3-PrD/1,2-PrD ratio. Ni-Cu/Re ratio was optimized to improve the catalytic activity. The best catalytic result, with 46 % 1,3-PrD yield and 1,3-PrD/1,2-PrD ratio of 1.24, was obtained when monometallic Ni catalyst at 40 wt % loading and modified with 7 wt % Re was used at 393 K, 5 MPa  $\text{H}_2$  pressure after 4 h of reaction. The overall 1,3-PrD yield starting from glycerol and assuming a two-step synthesis (Glycerol  $\rightarrow$  Glycidol  $\rightarrow$  1,3-PrD) and a yield of 78% for the first step, would be 36 %. This 1,3-PrD yield is the highest for non-noble metal catalyzed reaction and is comparable to direct hydrogenolysis of glycerol using noble metal catalysts, at longer time and high  $\text{H}_2$  pressure.

### Introduction

Biomass is a renewable source of organic carbon that is becoming important for the production of sustainable fuels and chemicals.<sup>[1]</sup> One of the most abundant biomass-related renewable materials is glycerol, which is generated during biodiesel production by transesterification of vegetable oils.<sup>[2]</sup> Biomass has higher O/C ratio than most valuable chemicals.<sup>[3]</sup> Hence, it is desirable to develop catalytic hydrogenolysis reaction to transform it into useful chemical products.<sup>[4]</sup> Hydrogenolysis catalysts should have the ability to activate hydrogen. Hydrogen can be activated on a metal surface. Typical metals used in hydrogenolysis include, nickel, copper and noble metals.<sup>[4c, 5]</sup>

Hydrogenolysis of glycerol has been widely studied. With most of the catalytic systems, the main product obtained was 1,2-propanediol (1,2-PrD).<sup>[6]</sup> However, the hydrogenolysis of glycerol

to 1,3-PrD is economically more attractive because 1,3-PrD is an important monomer in the synthesis of polypropylene terephthalate (PPT), a polymer that displays excellent properties.<sup>[7]</sup> Additionally, the current industrial production of 1,3-PrD is costly and involves the use of petrochemical based hazardous starting materials.<sup>[8]</sup> In a recent review by Nakagawa et al., tungsten-based materials or acid oxides, such as  $\text{ReO}_x$  or  $\text{MoO}_x$ , which are capable of activating glycerol were used as co-catalysts of several supported-noble metal catalysts in order to favor the formation of 1,3-PrD.<sup>[5b]</sup>

With respect to the use of W compounds, the presence of  $\text{H}_2\text{WO}_4$ , phosphotungstic acid ( $\text{H}_3\text{PW}_{12}\text{O}_{40}$ ), silicotungstic acid ( $\text{H}_4\text{SiW}_{12}\text{O}_{40}$ ) or  $\text{WO}_3$  in the catalysts favored the selectivity to 1,3-PrD.<sup>[9]</sup> This has been related to an increase of the amount of Brønsted acid sites in these catalysts.<sup>[10]</sup> The best result was obtained with a Pt- $\text{WO}_x/\text{Al}_2\text{O}_3$  catalyst that resulted in a selectivity to 1,3-PrD of 66% for a 64 % of conversion at 433 K and 5 MPa.<sup>[5b]</sup>

The role of  $\text{ReO}_x$  in improving the selectivity to 1,3-PrD was associated to the acidity of the -OH groups present on its surface, which are capable of activating glycerol.<sup>[11]</sup> Ir- $\text{ReO}_x/\text{SiO}_2$ <sup>[12]</sup> and Rh- $\text{ReO}_x/\text{SiO}_2$ <sup>[13]</sup> catalysts were tested for the hydrogenolysis of glycerol at 393 K in the presence of small amounts of mineral or solid acid additives. In the former catalyst, 1,3-PrD was obtained in 46% selectivity at 81% of conversion at 393 K, 8 MPa after 35 h while the later was equally active, but its selectivity to 1,3-PrD was much lower (14%).

In general, the selective hydrogenolysis of glycerol to 1,3-PrD requires expensive noble metal-based catalysts, high temperature and/or pressure and long reaction times. Even at these reaction conditions, the yield of 1,3-PrD was low or moderate.<sup>[5b]</sup> Hence, we propose the use of glycidol as an alternative to glycerol to obtain propanediols by catalytic hydrogenolysis, due to the high reactivity of glycidol and the fact that it could be readily obtained from glycerol.<sup>[14]</sup>

In the literature, the hydrogenolysis of tetrahydrofurfuryl alcohol (THFA), a cyclic ether with similar substitution pattern as glycidol, has been reported using Ir- $\text{ReO}_x/\text{SiO}_2$ <sup>[15]</sup>, Rh- $\text{ReO}_x/\text{SiO}_2$ <sup>[5b, 16]</sup>, and Rh- $\text{MoO}_x/\text{SiO}_2$ <sup>[17]</sup> catalysts. These catalysts led to 1,5-pentanediol (1,5-PD) with very high selectivity (> 90%). The mechanism of THFA hydrogenolysis involved adsorption of THFA, at the - $\text{CH}_2\text{OH}$  group, on the protonated  $\text{ReO}_x$  or  $\text{MoO}_x$  surface.  $\text{H}_2$  activated on the metal attacks C-O bond neighbouring the - $\text{CH}_2\text{OH}$  substituent and releases 1,5-PD.<sup>[15, 17a]</sup>

In our previous work on the hydrogenolysis of glycidol using mesoporous acid saponite supported Ni catalysts, it was observed that the presence of strong Brønsted acid sites improved the selectivity to 1,3-PrD.<sup>[18]</sup> The highest 1,3-PrD/1,2-PrD ratio was 0.97 at total conversion at 453 K using a catalyst with 40 wt % of Ni loading. In preliminary studies about the use

[a] Dr. F. B. Gebrestadik, Dr. P. Salagre, Dr. Y. Cesteros  
Dpt. Química Física i Inorgànica  
Universitat Rovira i Virgili  
C/ Marcel·lí Domingo s/n  
43007 Tarragona, Spain  
E-mail: pilar.salagre@urv.cat

[b] Dr. J. Llorca  
Institut de Tècniques Energètiques  
Universitat Politècnica de Catalunya  
Avda. Diagonal, 647  
08028 Barcelona (Spain)

## FULL PAPER

of bimetallic Ni-Cu catalysts we found that the Ni-Cu bimetallic catalyst at Ni: Cu atomic ratio 6:1 gave a better 1,3-PrD selectivity.

In this work, we modified several mesoporous acid saponite supported Ni, Cu mono- and bimetallic catalysts using various modifiers,  $\text{MO}_x$  (M = Mo, V, W and Re) in order to investigate their activity for the catalytic hydrogenolysis of glycidol. The effect of metal to modifier ratio was studied for  $\text{ReO}_x$ .

## Results and Discussion

## Characterization of the catalyst precursors and catalysts

XRD patterns of the Ni-Cu and modified Ni-Cu catalyst samples, after reduction at 623 K for 6 h, are displayed in Figure 1. All catalysts presented peaks at 19.4, 35.6 and 60.5°, 2 $\theta$ , corresponding to the (110, 020), (201) and (060) reflections of the saponite support and at 44.5 and 51.9°, 2 $\theta$ , related to the presence of metallic nickel. Broad or shoulder peaks observed in samples, Ni-CuMo(7)/MS, Ni-CuV(7)/MS and Ni-CuW(7)/MS (Figure 1 (b), (c) and (d), respectively) at 43.2 and 62.8°, 2 $\theta$ , were identified as NiO phase. Peaks corresponding to the modifiers or Cu were not observed in any sample, suggesting their small crystallite size or low crystallinity. In addition, there was no appreciable shift in the cell parameter of Ni in bimetallic catalysts and the formation of a Ni-Cu alloy was not clear from the XRD pattern. The presence of modifier seems to favor the dispersion of Ni, since the Ni crystallite size decreased from 27 nm to 11-21 nm in the presence of the modifiers (Table 1). The acidity of the modifiers and the basicity of the NiO phase and the subsequent acid-base interaction could justify this improved dispersion.

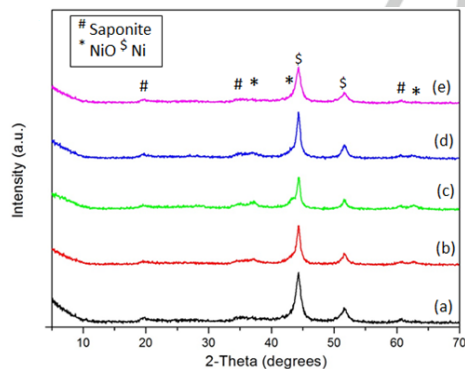


Figure 1. XRD patterns of Ni-Cu/MS samples with 40 wt % Ni-Cu loading (a) without modifier (b) Mo (c) V (d) W (e) Re modifier at 7 wt % loading.

Figure 2 shows the XRD patterns of supported monometallic Ni and Cu catalysts modified with Re and Ni-Cu bimetallic catalysts with different wt % of Ni-Cu loading and different modifier amount. For the monometallic modified Cu catalyst, sharp peaks were

observed at 43.3 and 50.4°, 2 $\theta$ , which were attributed to metallic copper crystalline phase. In the other samples, Ni phase was mainly observed and the Ni crystallite size increased when increasing the Ni-Cu wt % loading. For the catalysts prepared with lower Ni-Cu loading (30 and 20 wt%), (Ni-Cu\*Re(7)/MS and Ni-Cu\*\*Re(7)/MS), the peaks appeared broader and a shoulder was observed at about 43°, 2 $\theta$  indicating the presence of residual amounts of NiO (Figure 2(b) and (c), respectively). The Ni crystallite sizes of these two samples were 6 and 3 nm, respectively, in agreement with their lower metal loading. The value increased to 11 nm for Ni-CuRe(7)/MS. The other samples had comparable crystallite sizes (12-14 nm).

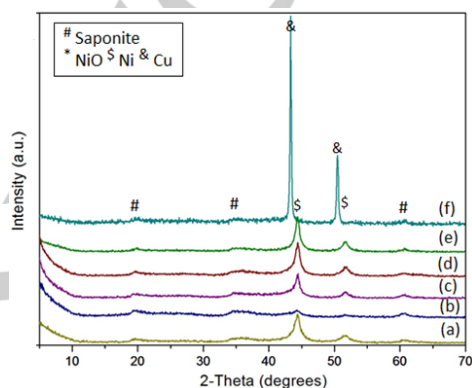


Figure 2. XRD patterns of (a) NiRe(7)/MS (b) Ni-CuRe\*(7)/MS (c) Ni-Cu\*Re(7)/MS (d) Ni-CuRe(3)/MS (e) Ni-CuRe(15)/MS (f) CuRe(7)/MS catalysts.

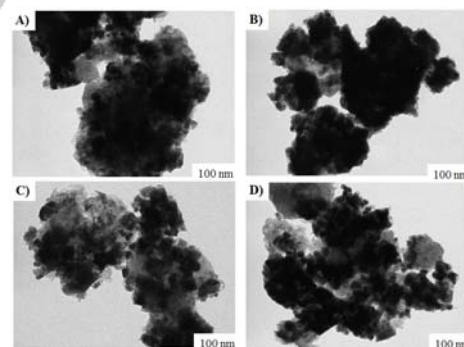


Figure 3. TEM images of A) Ni-Cu/MS B) Ni-CuMo(7)/MS C) Ni-CuRe(7)/MS and D) NiRe(7)/MS all at ~100 K.

Suprimit:

Suprimit:

Suprimit: 11

TEM microographies of the catalysts Ni-Cu/MS; Ni-CuMo(7)/MS; Ni-CuRe(7)/MS and Ni-CuV(7)/MS (Fig 3A, 3B, 3C and 3D respectively) allowed us to observe that the nickel particles sizes had similar values than the crystallite sizes obtained by XRD for these samples.

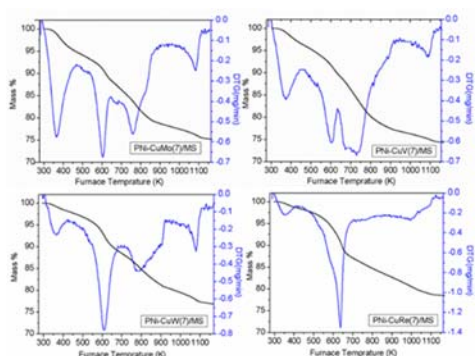


**Figure 4.** TGA results of cyclohexylamine treated samples of the modified catalyst precursors.

In order to explain the XRD results, it is necessary to have information about the interactions between NiO and CuO phases with the support and the modifiers, present in the precursors. Additionally, the acidity values of the catalytic precursors could be also interesting in order to have comparative information regarding the acidity of the catalysts. For these reasons, acidity and reducibility studies of the catalyst precursors were performed. Figure 4 displays the thermogravimetric analysis results of cyclohexylamine treated modified Ni-Cu catalyst precursors, used for the determination of the total surface acidity of the samples before reduction. The minima corresponding to the first derivative of the TGA curve can be associated to different processes related to the mass loss. Thus, those centred at about 350 and 1100 K, can be attributed to the water loss due to the dehydration of interlayer cations and dehydroxylation of the saponite structure, respectively. The other minima correspond to the mass loss associated with cyclohexylamine desorption. The number of these minima can be attributed to different acid sites while their temperature can be related to their acidity strength. Thus, the minima appeared at higher temperature correspond to stronger acid sites.

For PNi-CuMo(7)/MS, PNi-CuV(7)/MS and PNi-CuW(7)/MS catalyst precursors, two types of acid sites were observed. The minimum observed for all samples at about 600 K was similar to that of the unmodified catalyst precursor. This can be related to the acid sites of the support that were not influenced by the

modifiers. Another broader minimum, which appeared at an inflection point of about 750 K in these 3 modified catalyst precursors could be due to additional stronger acid sites associated to the presence of the modifiers. In contrast, for PNi-CuRe(7)/MS, mainly one minimum at 650 K was observed with only a small shoulder at around 600 K. It can be argued that Re, Ni and Cu oxides in PNi-CuRe(7)/MS are well dispersed, covering the main part of the support external surface, favouring the interaction of the H<sup>+</sup> of the support with the ReO<sub>x</sub>, resulting in mainly one type of acid sites with stronger acidity than that of the support without modifiers. The stronger acid sites detected in the catalyst precursors in the presence of modifiers could be associated with -OH groups [15] or with Lewis acid sites of the modifiers.

The TGA analysis results of cyclohexylamine treated Ni-Cu catalysts precursors at different wt % Ni-Cu loading and modified with different amounts of Re are displayed in figure 5. For catalyst precursors with 40 wt % Ni-Cu loading, the small minimum corresponding to the loss of CHA adsorbed on the acid sites of the support (600 K), appeared more defined at 3 and 15 wt % Re loading than at 7 wt %. When the Re loading was increased to 15 wt %, the position of the minimum related to the CHA adsorbed on the acid sites generated by the presence of modifiers shifted to higher temperature (700 K). This minimum also appeared at about 700 K for PNi-Cu\*Re(7)/MS and PNi-Cu\*\*Re(7)/MS. However, for these two samples, the mass loss due to desorption of CHA adsorbed on the acid sites corresponding to the support increased when decreasing the Ni-Cu loading. These results are consistent with the lower coverage of the support, when the Ni-Cu loading was lower.

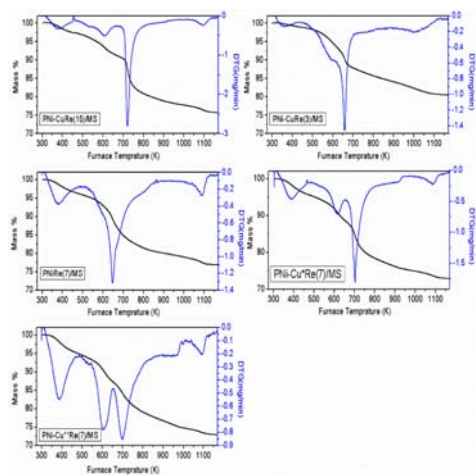
The total surface acidity of all the modified catalyst precursors was higher (1.45-2.03 mEq. CHA/g) than that of the unmodified Ni-Cu catalyst precursor (0.85 mEq. CHA/g) (Table 1). This confirms that modifiers provide an additional acidity. The values of total surface acidity increased with an increase in the amount of modifier or a decrease in the wt % of Ni-Cu loading.

NH<sub>3</sub>-TPD experiments were performed in selected catalysts precursor samples (Table 1) in order to supplement the results obtained from the CHA-TGA experiments. It was observed that the results obtained from the two methodologies are quite similar with the values slightly higher in the case of the NH<sub>3</sub> TPD. These results are in agreement with the mesoporosity of the saponite support and suggest that there was not any accessibility problem to the surface acid sites. The temperature-programmed reduction profiles of the unmodified Ni-Cu catalyst precursors and those modified with Mo, V, W and Re are displayed in figure 6. The temperature marked in the figure corresponds to the NiO reduction. However, the contribution of some modifier reduction cannot be discarded. The difference in the position of the NiO reduction peak should be consequence of its interaction with the support and/or with the modifiers, considering that NiO should be located between the support and modifiers taking into account the order of impregnation.

**Table 1.** Characterization results of the catalyst precursors and catalysts.

Catalyst Precursors	BET (m <sup>2</sup> /g)	Av. pore radius (Å)	Acidity [a] (mEq./g)	Acidity [b] (mEq./g)	Catalysts	Ni (NiO) [c] crystallite size (nm)
PNi-Cu/MS	220	27	0.96	1.02	Ni-Cu/MS	27
PNi-CuV(7)/MS	179	25	1.82	1.85	Ni-CuV(7)/MS	21 (3)
PNi-CuMo(7)/MS	156	26	1.69	1.75	Ni-CuMo(7)/MS	21 (6)
PNi-CuW(7)/MS	157	23	1.74	1.77	Ni-CuW(7)/MS	24 (4)
PNi-CuRe(7)/MS	340	31	1.88	—	Ni-CuRe(7)/MS	11
PNi-CuRe(3)/MS	347	31	1.45	—	Ni-CuRe(3)/MS	12
PNi-CuRe(15)/MS	268	34	1.92	—	Ni-CuRe(15)/MS	14
PNi-Cu*Re(7)/MS	362	30	1.95	2.06	Ni-Cu*Re(7)/MS	6
PNi-Cu**Re(7)/MS	429	33	2.03	2.13	Ni-Cu**Re(7)/MS	3
PNiRe(7)/MS	331	33	1.71	—	NiRe(7)/MS	13

Acidity in mEq. CHA/g of sample of the catalyst precursors from [a] TGA of cyclohexylamine (CHA) treated samples and [b] NH<sub>3</sub> TPD and [c] average crystallite size from XRD measurement.

**Figure 5.** TGA of cyclohexylamine treated catalyst precursors with different Re/Ni+Cu ratio.

For all the modified catalyst precursors, except for PNi-CuW(7)/MS, the main reduction peak was shifted to higher temperatures with respect to that corresponding to the unmodified one. This shift in the reduction temperature could be related to smaller NiO particles, interacting strongly with the support. This makes the reduction of the NiO more difficult. However, the shift for the sample with Re was very small (7 K). This lower shift is difficult to explain, but probably an opposite effect could take place in this sample favoring the reduction; this could be due to a decrease of the electronic density on the Ni(II) by interaction with the Re<sub>2</sub>O<sub>7</sub> phase, as will be discussed later. In this sample, additionally a well-defined peak was observed at

lower reduction temperature (530 K) that could be correlated with more effective NiO-Re<sub>2</sub>O<sub>7</sub> interactions in some particles.

For Ni-CuW(7)/MS, the main reduction peak was shifted to lower temperature by about 9 K. In our opinion, this should be more related to a certain decrease of the NiO particle size respect to the unmodified catalyst (from 27 to 24 nm) than to differences in interactions, since the degree of NiO dispersion was probably worse when the modifier was WO<sub>3</sub>. The higher size of the Ni particles in this catalyst when compared with that of the other modified catalysts is in agreement with this fact. This also agrees with the fact that this modifier is the oxide with less acidity.

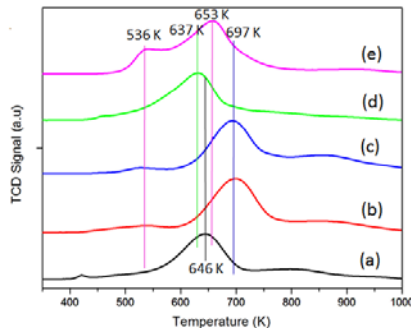
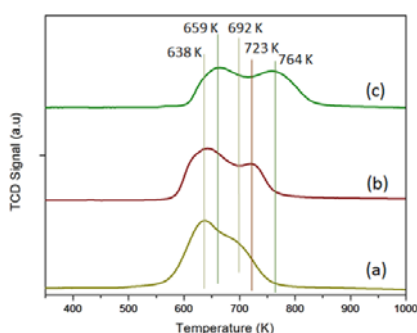
**Figure 6.** TPR profiles of Ni-Cu/MS catalyst precursors with 40 wt % of Ni-Cu loading (a) without modifier (b) Mo (c) V (d) W and (e) Re modifier at 7 wt % loading.

Figure 7 shows the reduction profiles of some catalyst precursors with different metal to Re ratio. The reduction of the modified monometallic Ni catalyst precursor, PNiRe(7)/MS, occurred in a broad interval (570-750 K) with two maxima, one more intense at 639 K, and other at 703 K. Comparing this graph with the curve corresponding to the modified bimetallic catalyst\_PNi-

CuRe(7)/MS of Fig 6(e), some part of NiO was easily reduced but other was more difficult to reduce. These differences in reducibility could be related to differences in NiO and Re<sub>2</sub>O<sub>7</sub> interactions. As previously commented, an effective NiO-Re<sub>2</sub>O<sub>7</sub> interaction should favor NiO reduction.



**Figure 7.** TPR profiles of the catalyst precursors (a) PNi(40)Re(7)/MS (b) PNi-Cu\*Re(7)/MS (c) PNi-Cu\*\*Re(7)/MS.

For the other Ni-Cu catalyst precursors prepared with 20 and 30 wt % total metal loading, the reduction peaks shifted to slightly higher temperatures. Two different reduction peaks were observed for both samples, which might stand for NiO particles with different interactions. The reducibility was more difficult for the precursor that after reduction presented the smallest Ni crystallite size (3 nm), probably due to a stronger interaction with the support. The reduction peaks at lower temperature, at 642 and 659 K for PNi-Cu\*Re(7)/MS and PNi-Cu\*\*Re(7)/MS, respectively, could be attributed to efficient NiO interactions with Re<sub>2</sub>O<sub>7</sub> that can favor its reduction. The lower reducibility of these samples could justify the presence of residual amounts of NiO.

The N<sub>2</sub>-physorption analysis results of the catalyst precursors are presented in table 1. The specific BET areas of all the catalyst precursors were lower than the BET area of the

support (600 m<sup>2</sup>/g)<sup>[19]</sup> indicating that some of the pore volume was occupied by the metal oxide particles. Comparing the BET areas of the unmodified catalyst precursor with the modified ones, they were lower for the V, Mo and W modified catalyst precursors. In contrast, for those modified with Re, the BET area was much higher (340 m<sup>2</sup>/g). This result suggested that Re can favor the dispersion of the metal oxide particles to a greater extent than the other modifiers. The smaller metal crystallite size of the corresponding reduced catalysts, determined by XRD, could support this fact, as will be discussed later.

At 3 wt % Re loading, the BET area was slightly higher (347 m<sup>2</sup>/g). However, when the Re loading was increased to 15 %, the BET area decreased to 268 m<sup>2</sup>/g. The BET area of the modified monometallic catalyst precursor, PNiRe(7)/MS (331 m<sup>2</sup>/g) was slightly lower than that of the bimetallic modified catalyst precursor, PNi-CuRe(7)/MS. This might indicate that the presence of Cu could assist the dispersion of Ni. The BET area values increased to 362 m<sup>2</sup>/g and 429 m<sup>2</sup>/g, respectively, when the amount of Ni-Cu loading decreased to 30 and 20 wt %, respectively. The average pore radius of all the catalyst precursors was in the mesoporous range (Table 1).

### Catalytic Activity

#### Influence of the type of modifier

The catalytic activity involves a complex interplay of competitive and/or cooperative metal and acid sites, as discussed later. For this reason, it was not possible to report catalytic rates in terms of turnover frequencies (TOF). Hence, in this work comparative catalytic activity results are presented based on conversion and selectivity.

Table 2 shows the catalytic activity results of Ni-Cu catalysts supported on a mesoporous acid saponite, modified with various types of acidic metal oxides. The activity should be a result of the metal and acid sites contribution, responsible for mainly hydrogenolysis and condensation reactions, respectively. These are competitive reactions. However, a cooperative effect of metal and acid sites could be expected in the hydrogenolysis reaction resulting in an increase of the selectivity to 1,3-PrD. This could take place by activation of glycidol, by H<sup>+</sup> interacting with the oxirane ring<sup>[11]</sup> or by interactions of acidic metal oxides MO<sub>x</sub> with the alcohol functionality of the glycidol.<sup>[19]</sup>

**Table 2.** Catalytic activity test results.

Catalyst	Conversion	Selectivity (%)				1,3-PrD/ 1,2-PrD	1,3-PrD yield (%)
		1,2-PrD	1,3-PrD	Propanol	Condensation products (dioxane/ dioxalane)		
CuRe(7)/MS	40	9	8	9	59	0.89	3.2
Ni-Cu/MS	73	47	15	5	21	0.33	11.0
Ni-CuMo(7)/MS	73	48	16	7	28	0.33	11.7
Ni-CuV(7)/MS	88	43	19	5	22	0.45	16.7
Ni-CuW(7)/MS	95	66	16	5	2	0.24	15.2
Ni-CuRe(7)/MS	98	45	34	8	8	0.76	31.6
Ni-CuRe(3)/MS	98	49	29	8	14	0.59	28.4
Ni-CuRe(15)/MS	98	42	35	6	13	0.83	34.3
Ni-Cu*Re(7)/MS	96	38	31	8	11	0.82	31.7
Ni-Cu**Re(7)/MS	98	35	31	7	13	0.89	33.3
NiRe(7)/MS	98	38	47	7	6	1.24	46.1

Re(7)/MS	47	n.d	n.d	59
----------	----	-----	-----	----

The total Ni-Cu loading in \* 30 wt% and \*\* 20 wt % in the other catalysts the total metal loading is 40 wt%. The Ni:Cu molar ratio in Ni-Cu bimetallic catalysts is 6:1.

All the modified samples showed comparable or higher activity than that of the unmodified catalyst. This might indicate that the modifiers could have a catalytic role either by acid activation of glycidol in the metal and H<sup>+</sup> cooperative route or as acid catalysts. The diol selectivity of these catalysts increased when W or Re were used as modifiers. This could be explained by the higher amount of metal phase, as a consequence of the higher reducibility of the corresponding catalyst precursors. For Mo and V modified catalysts, the propanediols selectivity was lower, in agreement with their lower NiO reducibility and the presence of residual amounts of NiO in the fresh catalysts.

All catalysts displayed comparable propanol selectivity suggesting that the formation of propanol was not related to high metal activity and was not the result of over hydrogenolysis of propanediols. The presence of propanol can be justified by the capacity of Cu to deoxygenate oxirane rings, as previously reported in the literature.<sup>[20]</sup> Regarding the condensation products selectivity (dioxane/dioxolane), the unmodified catalyst and those modified with Mo and V gave comparable selectivity (21-28%). The selectivity towards these products was lower for Re and W modified catalysts. These results agree with the higher metal activity of the later samples.

Regarding the 1,3-PrD/1,2-PrD ratio, the unmodified catalyst, Ni-Cu/MS, showed a value of 0.33. The value decreased in the case of W modified catalyst, was comparable in Mo modified catalyst, slightly higher for V modified catalyst and higher for Re modified catalyst (Table 2). The lower 1,3-PrD/1,2-PrD ratio (0.24) of Ni-CuW(7)/MS could be associated to Ni activity without acid collaboration, due to, probably a worse dispersion of WO<sub>3</sub> on the metal particles. For V and Re modified catalysts, the improved 1,3-PrD/1,2-PrD ratio might reflect the cooperation between acid and metal sites. This was especially the case for Re modified catalyst. The highest dispersion of the metal and the O-H groups of the ReO<sub>x</sub> phase makes possible this collaborative action. In general, among all the modified catalysts tested, the highest 1,3-PrD yield (31.6%) was obtained with Ni-Cu-Re (7)/MS catalyst.

#### Effect of Re to metal loading ratio

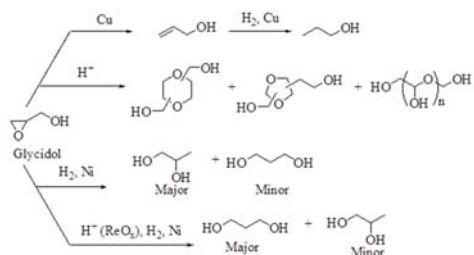
The effect of the amount of Re loading was studied in two ways; in one way, the amount of Re loading was varied (3, 7, 15 wt %) at constant Ni-Cu loading (40 wt %) and in the other, the Ni-Cu wt % loading was varied (20, 30 and 40 %) at constant Re loading (7 wt %).

The conversion was similar for all catalysts and was not significantly affected by the Re to metal ratio. The selectivity towards each of the products varied depending on the Re/Ni-Cu ratio. When the amount of Re loading increased at constant Ni-Cu loading, the 1,2-PrD selectivity decreased, the 1,3-PrD selectivity slightly increased, and hence the 1,3-PrD/1,2-PrD ratio increased. This might confirm that ReO<sub>x</sub> could be involved in the activation of glycidol leading to the formation of 1,3-PrD.

All the catalysts gave comparable propanol selectivity (6-8%) suggesting that its formation was neither related to acid sites nor to the hydrogenolysis activity of the metal. The selectivity to condensation products was higher at higher and lower Re loading. At higher Re/M molar ratio, this can be related to the higher and stronger acidity (Figure 3) while at lower Re loading, it could be associated with lower hydrogenolysis metal activity due to its lower NiO reducibility, as discussed earlier.

When Ni-Cu loading decreased (40, 30 and 20 wt %), the molar ratio Re/Ni-Cu increased, resulting in different catalytic behaviour. The propanediols selectivity slightly decreased and the 1,3-PrD/1,2-PrD ratio increased. The selectivity to condensation products increased when the Ni-Cu loading was lower. The reducibility of NiO was difficult and acidity was higher for samples with lower metal loading. Hence, the lower diol selectivity and higher condensation products selectivity could be explained by lower metal and higher acid activity, respectively. However, this increase of acidity had a positive effect to improve the selective formation of 1,3-PrD.

Monometallic Re modified Ni and Cu and the saponite support modified with Re without metal phase catalysts were prepared (NiRe(7)/MS, CuRe(7)/MS and Re(7)/MS) and their catalytic activity was tested for comparison (Table 3). Re modified Ni catalyst showed the highest selectivity to propanediols (85%) and 1,3-PrD (47 %) with the highest 1,3-PrD/1,2-PrD ratio (1.24) and low condensation products selectivity. The high 1,3-PrD selectivity could be related to an effective collaborative action between metal and acid sites. On the other hand, the modified Cu catalyst afforded the lowest propanediol selectivity, higher propanol selectivity and the highest condensation products selectivity. This might reflect the poor hydrogenolysis activity of Cu at the conditions used, and the high activity of the acid sites. The propanol, as discussed earlier, is the result of Cu catalysed deoxygenation reaction of the epoxide ring followed by hydrogenation of the resulting double bond. Re modified support showed comparable moderate activity as that of the modified Cu catalyst with identical condensation products selectivity. This confirms the previous argument that condensation products can be related to acid sites. The major reaction pathways of the acid and metal catalysed reactions, discussed above, are summarized in scheme 1.



**Scheme 1.** The major reaction pathways of acid and/or metal catalyzed reactions of glycidol.

In summary, among all the modified catalysts tested, Re modified catalysts showed higher activity, propanediols selectivity and 1,3-PrD/1,2-PrD ratio. The experiments about Re/M ratio revealed that the optimum modifier and active metal loading was obtained for the monometallic Ni catalyst at 40 wt % loading and when the Re content was 7 wt %. The activity test at this optimum composition, catalyst NiRe(7)/MS, at 393 K gave 1,3-PrD in 46.1 % yield with a 1,3-PrD/1,2-PrD ratio of 1.24 at 98 % of conversion after 4 h of reaction.

#### XPS study: Ni-CuRe(7)/MS vs NiRe(7)/MS catalysts

In order to better understand the differences in the catalytic behaviour of NiRe(7)/MS and Ni-CuRe(7)/MS catalysts, three XPS experiments were designed. Samples were prepared and analyzed as described in the experimental section. The first group of samples were named as fresh catalysts, since they were the catalysts obtained just after reduction and before reaction. However, in these samples some degree of oxidation could be

expected during catalyst handling for the XPS analysis. The second group of samples were the catalysts, which were activated by reduction in-situ with H<sub>2</sub> at 623 K for 30 min, and the third group of samples were the spent catalysts, which were obtained after being used in the catalytic test and without any treatment. The XPS of the support modified with ReO<sub>x</sub> without metal, Re/MS, was also performed for comparison. The binding energies of the characteristics XPS peaks are summarized in table 3.

The surface composition of the fresh and spent samples was compared to that of the theoretical composition of the catalysts (Table 3). Regarding the ratio between Ni and Cu, the nominal bulk values of the catalyst was Ni:Cu=6:1 by weight, which corresponds to an atomic ratio of Cu/Ni=0.16. The fresh sample Ni-CuRe(7)/MS exhibited a surface atomic ratio of Cu/Ni close to this value, 0.15, which means that Ni and Cu are both equally dispersed on the surface. The spent sample showed a slightly higher Cu/Ni ratio of 0.19, indicating a slight enrichment of Cu at the surface during reaction. In the H<sub>2</sub> activated sample, the Cu/Ni surface atomic ratio increased considerably up to 0.28, indicating segregation of Cu towards the surface. The theoretical Re/(Ni+Cu) atomic ratio was approximately 0.052 for samples NiRe(7)/MS and Ni-CuRe(7)/MS. The values of the Re/(Ni+Cu) atomic ratios at the surface measured by XPS were 0.031 in NiRe(7)/MS and 0.047 in Ni-CuRe(7)/MS, in the fresh samples. This means that the dispersion of Re was good especially when Cu was present in the catalyst. For NiRe(7)/MS catalyst, it could be possible that Re was decorated by Ni. Interestingly, the spent samples showed comparable Re/(Ni+Cu) atomic ratios than the fresh ones, 0.039 and 0.045. In contrast, the samples reduced in-situ at 623 K had lower Re/metal atomic ratios, 0.020 Re/Ni and 0.029 Re/(Ni+Cu). The decoration of ReO<sub>x</sub> by the Ni particles could explain a best collaborative effect between Ni and ReO<sub>x</sub> in the reaction, which is considered responsible for the observed 1,3-PD production with NiRe(7)/MS.

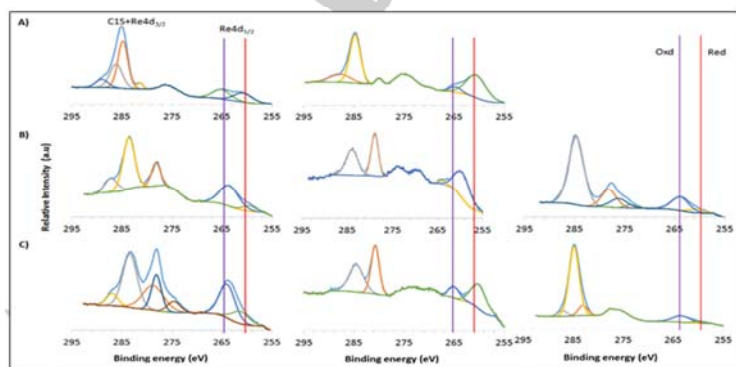


**Figure 8.** Re 4d spectra of A) fresh and H<sub>2</sub> activated Re(7)/MS and fresh, H<sub>2</sub> activated and spent catalysts, from left to right, of B) NiRe(7)/MS and C) Ni-CuRe(7)/MS. The red line indicates the position of Re in a low oxidation state whereas the blue one indicates the position of oxidized Re, both corresponding to 4d<sub>5/2</sub> photoelectrons. The 4d<sub>5/2</sub> peaks are overlapped to the C 1s photoelectrons.

The Re 4d spectra of the different catalysts as prepared (fresh), after in-situ H<sub>2</sub> activation at 623 K, and after reaction (spent) are displayed in figure 8. The spectra of Re correspond to the 4d<sub>5/2</sub> peaks, since the 4d<sub>3/2</sub> peaks are superposed to the C 1s photoelectrons. All the spectra showed two components corresponding to two different oxidation states for Re. The red line indicates the position of the Re 4d<sub>5/2</sub> photoelectrons corresponding to the lower oxidation state whereas the blue one indicates the position of the Re 4d<sub>5/2</sub> photoelectrons corresponding to the higher oxidation state. In the fresh samples, Re was mainly in the higher oxidation state for NiRe(7)/MS and Ni-CuRe(7)/MS catalysts, whereas in the Re(7)/MS sample the contribution of the less oxidized form was more important. After in situ H<sub>2</sub> activation at 623 K, Re became less oxidized, but there was always a component of highly oxidized Re (probably VI or VII). It is interesting to note that the reduction degree of Re was similar for samples Re and NiRe(7)/MS (88-93%), but in the sample Ni-CuRe(7)/MS, Re was much more difficult to reduce (after reduction there was about 75% Re reduced to lower oxidation state). Probably, the Cu-Re interaction favors the electronic transfer from Re to Cu, increasing the oxidation state of Re. The spent samples exhibited both Re species, in similar amounts as in the corresponding fresh samples.

Considering the real catalysts, from the commented XPS results, it is possible to argue that there is a higher amount of Re

with higher oxidation state in Ni-CuRe(7)/MS catalyst compared to NiRe(7)/MS catalyst. This might result in a higher acid activity of the catalyst, Ni-CuRe(7)/MS, according to the observed products distribution.

Figure 9 shows the Ni 2p spectra for the fresh, activated and spent (NiRe(7)/MS and Ni-CuRe(7)/MS) samples. The fresh samples exhibited similar Ni spectra, with Ni mainly oxidized, but with the presence of a minor component of reduced Ni as well. After in-situ H<sub>2</sub> activation at 623 K, Ni was reduced considerably, but not totally. It is interesting to highlight that a significant fraction of Ni was still oxidized after the in-situ reduction in the Ni-CuRe(7)/MS sample (about 75% of oxidized Ni). In contrast, the degree of Ni reduction was much higher in the sample without Cu, the NiRe(7)/MS sample (about 57% of oxidized Ni). This fact, together with the difficulty of reducing Re in the Ni-CuRe(7)/MS sample during the in-situ reduction treatment, as pointed out above, suggests that the presence of Cu strongly interacting with both Re and Ni and that Cu prevents both Re and Ni reduction. This is likely an electronic donation from Re and Ni towards Cu. Finally, the Ni spectra of NiRe(7)/MS and Ni-CuRe(7)/MS spent samples were virtually identical and similar to the corresponding fresh samples. These experiments showed that in the catalyst without Cu, NiRe(7)/MS, there was a higher amount of reduced Ni, which in turn can be correlated with its higher propanediol selectivity.

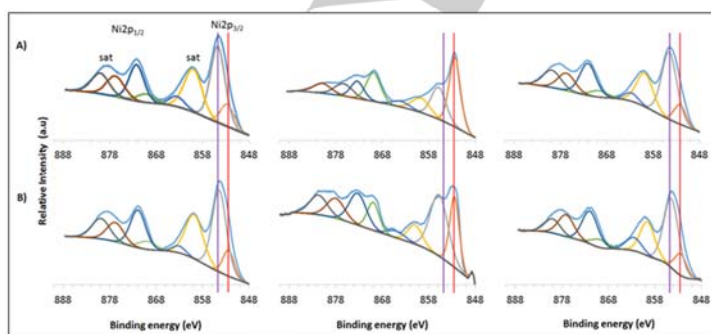


**Figure 9.** Ni 2p spectra of the fresh, H<sub>2</sub> activated and spent catalysts, from left to right of A) NiRe(7)/MS and B) Ni-CuRe(7)/MS. The red line indicates the position of reduced Ni whereas the blue one indicates the position of oxidized Ni (2p<sub>3/2</sub> photoelectrons).

**Table 3.** XPS analysis results of selected fresh, H<sub>2</sub> activated and spent catalysts.

Catalyst	Binding energies (eV) of characteristic peaks			Re/ Ni-Cu	Ni/Cu	Ni(Red)/ Ni (Ox)	Cu(Red)/ Cu(Ox)
	Ni	Cu	Re				
Re/MS-fresh	—	—	Ox 4d <sub>5/2</sub> -265.1 Red 4d <sub>5/2</sub> -260.8	—	—	—	—
Re/MS- H <sub>2</sub> act.	—	—	Ox 4d <sub>5/2</sub> -264.8 Red 4d <sub>5/2</sub> -260.6	—	—	—	—
Ni-CuRe(7)/MS-fresh	Ni <sup>2+</sup> 2p <sub>3/2</sub> -852.4 Ni <sup>3+</sup> 2p <sub>3/2</sub> -854.4	Cu <sup>2+</sup> 2p <sub>3/2</sub> -933.1 Cu <sup>1+</sup> 2p <sub>3/2</sub> -931.1	Ox 4d <sub>5/2</sub> -263.9 Red 4d <sub>5/2</sub> -260.6	0.047	0.15	0.14	1.14

Ni-CuRe(7)/MS- H <sub>2</sub> act.	Ni <sup>2+</sup> 2p <sub>3/2</sub> -852.5 Ni <sup>2+</sup> 2p <sub>3/2</sub> -855.8	Cu <sup>2+</sup> 2p <sub>3/2</sub> -928.5 Cu <sup>2+</sup> 2p <sub>3/2</sub> -931.7	Ox 4d <sub>5/2</sub> -263.5 Red 4d <sub>5/2</sub> -260.6	0.029	0.28	0.15	1.76
Ni-CuRe(7)/MS-spent	Ni <sup>2+</sup> 2p <sub>3/2</sub> -852.5 Ni <sup>2+</sup> 2p <sub>3/2</sub> -854.5	Cu <sup>2+</sup> 2p <sub>3/2</sub> -932.7 Cu <sup>2+</sup> 2p <sub>3/2</sub> -932.2	Ox 4d <sub>5/2</sub> -263.8 Red 4d <sub>5/2</sub> -259.5	0.045	0.19	0.45	3.60
NiRe(7)/MS-fresh	Ni <sup>2+</sup> 2p <sub>3/2</sub> -852.6 Ni <sup>2+</sup> 2p <sub>3/2</sub> -854.7	—	Ox 4d <sub>5/2</sub> -263.4 Red 4d <sub>5/2</sub> -260.0	0.031	—	0.15	—
NiRe(7)/MS- H <sub>2</sub> act.	Ni <sup>2+</sup> 2p <sub>3/2</sub> -852.4 Ni <sup>2+</sup> 2p <sub>3/2</sub> -855.9	—	Ox 4d <sub>5/2</sub> -263.9 Red 4d <sub>5/2</sub> -261.3	0.020	—	0.13	—
NiRe(7)/MS-spent	Ni <sup>2+</sup> 2p <sub>3/2</sub> -852.3 Ni <sup>2+</sup> 2p <sub>3/2</sub> -854.6	—	Ox 4d <sub>5/2</sub> -265.0 Red 4d <sub>5/2</sub> -261.0	0.039	—	0.96	—

The total Ni-Cu loading in \* 30 wt% and \*\* 20 wt % in the other catalysts the total metal loading is 40 wt%. The Ni:Cu molar ratio in Ni-Cu bimetallic catalysts is 6:1.

Figure 10 shows the Cu 2p spectra for the sample Ni-CuRe(7)/MS as well as the Cu LMM Auger lines. In the fresh sample both reduced and oxidized Cu can be observed. However, after in situ H<sub>2</sub> activation at 623 K the spectrum changed dramatically and Cu was strongly reduced (about 78%). This was also clearly observed in the Auger lines, where the peaks at 334.9 and 332.0 eV clearly showed the presence of metallic Cu. It is outstanding the absence of satellite lines and the appearance of two different reduced Cu species after the in situ reduction treatment in the Cu 2p spectra. At this point it is difficult to unambiguously identify the nature of these two species. One of

the components may correspond to metallic Cu and the other one can be assigned to a Cu-M interaction. In fact, the electron donation from Re and Ni towards Cu in the Ni-CuRe(7)/MS sample, discussed above, agrees with the observed strongly reduced component in the Cu 2p spectrum, which is compatible with the existence of a type of Cu that acts as an electron acceptor. Finally, for the spent sample the spectrum was similar to that of the fresh one, although the lower intensity of the satellite lines in the 2p spectrum indicates a slightly higher reduction character in the spent sample.

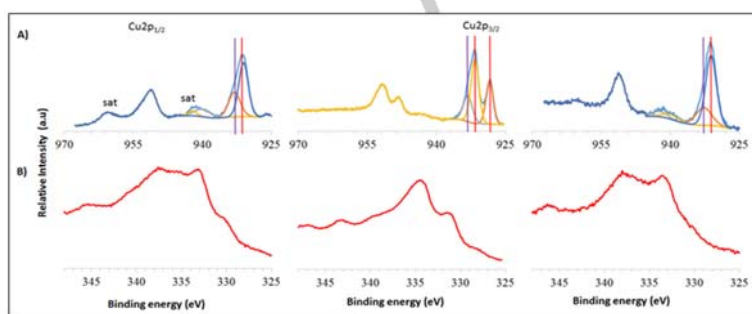


**Figure 10.** Cu 2p (A) and Auger Cu LMM (B) spectra of fresh, H<sub>2</sub> activated and spent Ni-CuRe(7)/MS catalyst. The red line indicates the position of reduced Cu whereas the blue one indicates the position of oxidized Cu (2p<sub>3/2</sub> photoelectrons). In addition, Cu(II) species are accompanied by satellite lines (sat).

## Conclusions

Ni-Cu catalysts prepared at 40 wt % total metal loading were modified with 7 wt % Mo, V, W and Re loading. Some catalysts at different Ni-Cu/Re ratio and Re modified monometallic Ni and Cu catalysts, were also prepared for comparison. The characterization results revealed that the presence of vanadium and molybdenum modifiers made the reduction of NiO more difficult. The reducibility of NiO got harder when the amount of metal loading was lower. Total surface acidity and acidity strength increased in the presence of modifiers, with an increase in the

amount of modifier and with a decrease in the amount of metal loading. BET area and XRD analysis confirmed that the dispersion of the NiO and the Ni in the catalyst precursors and catalysts, respectively, increased in the presence of modifiers and with a decrease in the amount of Ni-Cu loading. The dispersive effect was higher in the presence of Re modifier.

The catalytic activity of all the modified catalysts was comparable or higher than the unmodified catalysts. The presence of V and Re modifier increased the 1,3-PrD and 1,2-PrD ratio to 0.45 and 0.7, respectively when compared to the unmodified catalyst (0.33) or to those modified with W (0.24) or Mo (0.33). The results confirmed that Re plays an important role in improving the 1,3-PrD production. The W modified catalyst

**Table 4.** Nomenclature, type of modifier, amount of metal and modifier loading of the catalysts.

Catalysts	Total Ni-Cu wt % loading	Modifier M (MOx)	Modifier wt %
Ni-Cu/MS	40	—	—
Ni-CuV(7)/MS	40	V	7
Ni-CuMo(7)/MS	40	Mo	7
Ni-CuW(7)/MS	40	W	7
Ni-CuRe(7)/MS	40	Re	7
Ni-CuRe(3)/MS	40	Re	3
Ni-CuRe(15)/MS	40	Re	15
Ni-Cu*Re(7)/MS	30	Re	7
Ni-Cu**Re(7)/MS	20	Re	7
NiRe(7)/MS	40	Re	7
CuRe(7)/MS	40	Re	7

gave the highest selectivity to propanediol (82%), the lowest selectivity to condensation products (2%), and the lowest 1,3-PrD/1,2-PrD ratio, in agreement with its high NiO reducibility and hence metal activity.

The important role of Re modifier was confirmed by the increase of 1,3-PrD/1,2-PrD ratio when Re/ Ni + Cu ratio increased by increasing the Re content or decreasing the Ni-Cu loading. However, at lower metal loading the diol selectivity was lower and the selectivity to the condensation products was higher as would be expected from the low NiO reducibility and high acidity of these samples. The monometallic Cu catalysts gave the lowest propanediol and the highest condensation products selectivity comparable to that of the Re modified support without an active metal. This confirmed the lower hydrogenolysis capacity of Cu in the catalytic system. The Re modified Ni catalysts showed high 1,3-PrD/1,2-PrD ratio (1.24), high propanediol selectivity and the highest 1,3-PrD yield (46.1%) of all the catalysts studied. These results can be explained by some decoration of the Ni particles by the ReO<sub>x</sub>, as can be deduced from XPS results, that favor the collaborative action between the metal sites and ReO<sub>x</sub> responsible for the 1,3-PrD production. The yield of 1,3-PrD obtained in this work was comparable or higher than those previously reported in the literature for the hydrogenolysis of glycerol, using noble metal catalysts, at harsh reaction conditions and longer reaction times.

## Experimental Section

### Preparation of supported catalysts

Mesoporous saponite in the H<sup>+</sup> form (MS) (surface acidity, 1.02 mEq H<sup>+</sup>/g) synthesized as previously reported by our research group<sup>[19]</sup>, was used as support for catalyst preparation. MS was stable until 1035 K, (temperature of clay dehydroxylation), as determined by TGA.<sup>[19]</sup> Ni-Cu/MS catalysts with 20, 30 and 40 wt % total metal loading, and Ni: Cu wt % ratio 6:1 were prepared by impregnation of 1 g of the support with a calculated volume of 0.5 M Ni-Cu in ethanol solution containing appropriate amounts of Ni(NO<sub>3</sub>)<sub>2</sub> and Cu(NO<sub>3</sub>)<sub>2</sub> salts. After removing the solvent by rotary evaporation and drying at 383 K overnight, the samples were calcined at 723 K for 5 h.

Several Ni-Cu-MO<sub>x</sub>/MS (M = W, Mo, V and Re) catalysts were prepared by impregnating the Ni-Cu/MS (prepared at 40 wt % Ni-Cu loading) with an aqueous solution of the modifier metal precursors, (NH<sub>4</sub>)<sub>10</sub>W<sub>12</sub>O<sub>41</sub>·4H<sub>2</sub>O, (NH<sub>4</sub>)<sub>6</sub>Mo<sub>7</sub>O<sub>24</sub>·4H<sub>2</sub>O, NH<sub>4</sub>VO<sub>3</sub> and NH<sub>4</sub>ReO<sub>4</sub>. The amount of MO<sub>x</sub> modifier expressed per mass of W, Mo and V respect to unmodified catalyst was 7 wt %. The amount of Re loading was varied at

3, 7 and 15 wt %, resulting in catalysts, Ni-CuRe(3)/MS, Ni-CuRe(7)/MS and Ni-CuRe(15)/MS, with molar ratio values (M/Re) of 42, 18 and 8 respectively.

The effect of Ni-Cu/Re wt % ratio was also studied by decreasing the metal loading at 30 and 20 wt % Ni-Cu wt % and maintaining the Re loading as in the Ni-CuRe(7)/MS catalyst. This was performed in order to increase the acid contribution of the support by decreasing the support acid site coverage. The resulting catalysts were labelled as Ni-Cu\*Re(7)/MS and Ni-Cu\*\*Re(7)/MS, for 30 and 20% of metal loading, respectively. The (Ni + Cu)/Re molar ratios for these catalysts were 13 and 9. Monometallic Ni and Cu catalysts were prepared at 40 wt % metal loading and modified with 7 wt % Re, for comparison.

All catalysts were reduced in a tubular reactor under hydrogen flow (75 mL/min) at 623 K for 6 h. The preparation conditions and nomenclature of the catalysts are summarized in table 1. The catalyst precursors were labelled with P at the beginning of the name.

### Catalysts characterization

X-ray diffractogram (XRD) patterns of powdered catalyst samples were recorded on a Siemens D5000 diffractometer equipped with a CuK $\alpha$  radiation ( $\lambda = 1.54$  Å) source. Measurements were done in 2 $\theta$  diffraction angle between 5 and 70°, with an angular step of 0.05° and at rate of 3 s per step. Crystalline phases were identified by cross comparison of the diffractogram of the sample with a reference data from international centre for diffraction data (JCPDS files). Integral breadth estimated by fitting intense reflection peaks of metal or metal oxide particles and by applying TOPAS 4.1, was used to calculate the crystallite sizes using the Scherrer equation.

N<sub>2</sub> adsorption-desorption analysis was performed on Quadrasorb sorptometer at liquid nitrogen temperature (77 K) to determine the specific BET area and porosity. Before measurement, samples (~0.1 g) were degassed overnight at 383 K. Specific surface area was determined by applying the BET method and the pore size distribution was estimated by BJH method.

TEM characterization was done using JEOL 1011 transmission electron microscope operating at an accelerating voltage of 100 kV and magnification of 200 k. Sample (0.1 mg) was dispersed in ethanol (50  $\mu$ L) with the aid of an ultrasounds. Then, it was deposited on a carbon coated copper grid and air dried.

Temperature-programmed reduction of the catalyst precursors was measured by an Autochem AC2920 Micrometric apparatus. The catalyst precursor sample, calcined beforehand (0.1 g), was placed in a tubular reactor and heated between room temperature and 1173 K at a rate of 10 K/min under a flow of 5 vol.% H<sub>2</sub> in argon (50 mL/min). The hydrogen consumption was controlled by a TCD detector.

Total surface acidity of the catalyst precursors was determined by thermogravimetric analysis (TGA) of cyclohexylamine treated samples (~0.1 g) following the protocol described by Mokaya *et al.*<sup>[21]</sup> The analysis was conducted in a Labsys Setaram TGA microbalance equipped with a programmable temperature furnace. Each sample was heated under N<sub>2</sub> flow (80 cm<sup>3</sup>/min) from 303 to 1173 K at a rate of 5 K/min. The total acidity was equivalent to the amount of cyclohexylamine (CHA) desorbed at the temperature range of 523-923 K in which the sample without cyclohexylamine treatment did not show any significant mass loss.<sup>[19]</sup>

Several NH<sub>3</sub>-TPD experiments were performed on selected catalyst precursors to complement the acidity results obtained by CHA-TGA analysis, and to compare the relative contribution of external and internal acid sites. The analysis was conducted on AC2920 apparatus. In a typical experiment, about 0.2 g, sieved catalyst precursor sample was loaded in U-shaped quartz tube and submitted to surface pre-treatment under a flow of He at 623 K for 1 h. It was then cooled down to 373 K and saturated with pure NH<sub>3</sub> for 30 min. The physically adsorbed NH<sub>3</sub> was removed by purging the sample with pure He for 30 min and the sample was heated

Suprimit :

from 373 to 973 K at a heating rate of 10 K/min and the NH<sub>3</sub> desorption was monitored with a TCD detector. The peak area of detected TPD peak was correlated with the amount of desorbed NH<sub>3</sub> on the basis of pulsed NH<sub>3</sub> injection experiment and the total surface acidity was predicted from the amount of ammonia desorbed.

Surface characterization of some fresh, spent and H<sub>2</sub> in-situ activated catalysts was performed by X-ray photoelectron spectroscopy (XPS) on a SPECS system equipped with an Al anode XR50 source operating at 150 mW and a Phoibos MCD-9 detector. The pressure in the analysis chamber was always kept below 10<sup>-7</sup> Pa. The area analyzed was about 2 mm x 2 mm. The pass energy of the hemispherical analyzer was set at 25 eV and the energy step was fixed at 0.1 eV. Powdered samples were pressed to self-supported pellets. In-situ experiments were performed under dynamic conditions in an adjacent chamber at atmospheric pressure equipped with a mass spectrometer and an IR lamp to heat the sample. The sample was transferred under ultra-high vacuum between the in-situ chamber and the analysis chamber. Gases were accurately dosed into the in-situ chamber by using mass flow controllers, and the temperature was measured by using a K-type thermocouple in contact with the sample holder. Data processing was performed with the CasaXPS program (Casa Software Ltd., UK). The binding energy (BE) values were referred to the C 1s peak at 284.8 eV. Atomic fractions were calculated using peak areas normalized on the basis of acquisition parameters after background subtraction, experimental sensitivity factors and transmission factors provided by the manufacturer.

#### Catalytic activity test

Activity test was performed in a 50 mL stainless steel autoclave equipped with an electronic temperature controller and a mechanical stirrer. Glycidol (3.77 mL) was dissolved in sulfolane (30 mL) and purged with nitrogen and 1 g of freshly reduced catalyst was carefully transferred into the reactor under a positive nitrogen pressure to avoid contact with atmosphere. The reactor was sealed, purged three times with 4 MPa N<sub>2</sub> pressure and three times with 1 MPa H<sub>2</sub> pressure. After performing a leakage test, the temperature of the reaction was set at 393 K. The reaction mixture was vigorously stirred at 600 rpm. This together with the use of powdered catalysts and the mesoporous nature of the support used for catalyst preparation avoids internal and external mass and heat transfer limitations and diffusion problems. When the temperature in the electronic control read the final temperature of the reaction, the hydrogen pressure was adjusted at 5 MPa and the reaction time was started (t<sub>0</sub>). The reaction was run for 4 h while feeding hydrogen on demand. At the end of the reaction time (t<sub>f</sub>), the mixture was cooled down and the reaction products were separated from the catalyst by filtration. Liquid products were analysed on Shimadzu GC-2010 chromatography using SupraWAX-280 capillary column, 1-butanol as internal standard and FID detector. Some liquid samples were submitted for GC-MS analysis to identify unknown products. Conversion and selectivity were calculated according to the following equations:

$$\text{Conversion} = \frac{(\text{moles of glycidol @ } t_0 - \text{moles of glycidol @ } t_f)}{\text{moles of glycidol } t_0} * 100\%$$

$$\% \text{ Selectivity } x = \frac{\text{moles of } x * \# \text{ carbon in } x}{(\text{mole glycidol @ } t_0 - \text{mole glycidol @ } t_f) * 3} * 100\%$$

Where t<sub>0</sub> and t<sub>f</sub> are the initial and the final times, respectively.

#### Acknowledgements

The authors are grateful for the financial support of the Ministerio de Economía y Competitividad of Spain and FEDER funds

(CTQ2011-24610). J. Llorca is Serra Hünter Fellow and is grateful to ICREA Academia program.

**Keywords:** glycidol • hydrogenolysis • nickel • metal oxide modifier • propanediol • bifunctional catalyst

- [1] a) M. Schlaf, Dalton Trans. **2006**, 4645-4653. b) A. Corma, S. Iborra, A. Velty, Chem. Rev. **2007**, 1072411-2502. c) P. C. A. Bruijninx, Ramán-Leshkov, Catal. Sci. Technol. **2014**, 4, 2180-2181.
- [2] C.-H. Zhou, J. N. Beltrami, Y.-X. Fan, G. Q. Lu, Chem. Soc. Rev., **2008**, 37, 527-549.
- [3] a) R.M. West, E.L. Kunkes, D.A. Simonetti, J.A. Dumesic, Catal. Today, **2009**, 147, 115-125. b) A. Yamaguchi, N. Hiyoshi, O. Sato, K.K. Bando, M. Shirai, Green Chem. **2009**, 11, 48-52.
- [4] a) Y. Nakagawa, K. Tomishige, Catal. Sci. Technol. **2011**, 1, 179-190. b) S. Sittithisa, T. Sooknoi, Y. Ma, P.B. Balbuena, D.E. Resasco, J. Catal. **2011**, 277, 1-13. c) K.L. Deutsch, B.H. Shanks, J. Catal. **2012**, 285, 235-241.
- [5] a) P. Maki-Arvela, J. Hájek, T. Salmi, D. Y. Murzin, Appl. Catal., A, **2005**, 292, 1-49. b) Y. Nakagawa, M. Tamura, K. Tomishige, J. Mater. Chem. A, **2014**, 2, 6688-6702.
- [6] a) M. A. Dasari, P.-P. Kiatsimkul, W. R. Sutterlin, G. J. Suppes, Appl. Catal., A, **2005**, 281, 225-231. b) Y. Kusunoki, T. Miyazawa, K. Kunimori, K. Tomishige, Catal. Commun. **2005**, 6, 645-649. c) T. Miyazawa, S. Koso, K. Kunimori, K. Tomishige, Appl. Catal., A, **2007**, 329, 30-35. d) J. Feng, J. Wang, Y. Zhou, H. Fu, H. Chen, X. Li, Chem. Lett., **2007**, 36, 1274-1275. e) T. Sánchez, P. Salagre, Y. Cesteros, A. B. López, Chem. Eng. J. **179** (2012) 302-311.
- [7] a) P. N. Caley, R. C. Everett, Patent US 3350871, **1967**, DuPont. b) D. Zimmerman, R. B. Isaacson, Patent US 3814725, **1974**, Celanese Corp.
- [8] A. Peroša, P. Tundo, Ind. Eng. Chem. Res. **2005**, 44, 8535-8537.
- [9] a) T. Kurosaka, H. Maruyama, I. Naribayashi, Y. Sasaki, Catal. Commun. **2008**, 9, 1360-1363. b) J. Chaminand, L. Djakovitch, P. Gallezot, P. Marion, C. Pinel, C. Rosier, Green Chem. **2004**, 6, 359-361. c) N. Suzuki, Y. Yoshikawa, M. Takahashi, M. Tamura, World Pat. 2007129560, **2007**, KAO Corporation. d) E. I. Ross-Medgaarden, W. V. Knowles, T. Kim, M. S. Wong, W. Zhou, C. J. Kiely, I. E. Wachs, J. Catal. **2008**, 256, 108-125. e) L. Liu, Y. Zhang, A. Wang, T. Zhang, Chin. J. Catal. **2012**, 33, 1257-1261. f) J. ten Dam, K. Djanashvili, F. Kapteijn, U. Hanefeld, ChemCatChem. **2013**, 5, 497-505. g) R. Arundhati, T. Mizugaki, T. Mitsudome, K. Jitsukawa, K. Kaneda, ChemSusChem. **2013**, 6, 1345-1347. h) S. Zhu, X. Gao, Y. Zhu, Y. Li, J. Mol. Catal. A: Chem. **2015**, 398, 391-398. i) S. Zhu, Y. Qiu, Y. Zhu, S. Hao, H. Zheng, Y. Li, Catal. Today **2013**, 212, 120-126. j) S. Zhu, X. Gao, Y. Zhu, J. Cui, H. Zheng, Y. Li, Appl. Catal., B, **2014**, 158-159, 391-399.
- [10] L. Gong, Y. Lu, Y. Ding, R. Lin, J. Li, W. Dong, T. Wang, W. Chen, Appl. Catal., A, **2010**, 390, 119-126.
- [11] M. Chia, Y. J. Pagán-Torres, D. Hibbitts, Q. Tan, H. N. Pham, A. K. Datye, M. Neurock, R. J. Davis, J. A. Dumesic, J. Am. Chem. Soc. **2011**, 133, 12675-12689.
- [12] Y. Nakagawa, Y. Shinmi, S. Koso, K. Tomishige, J. Catal. **2010**, 272, 191-194.
- [13] K. Chen, S. Koso, T. Kubota, Y. Nakagawa, K. Tomishige, ChemCatChem. **2010**, 2, 547-555.
- [14] a) W. Yoo, Z. Mouloungui, A. Gaset, USP 6316641, **2001**. b) R. Bai, H. Zhang, F. Mei, S. Wang, T. Li, Y. Gu and G. Li, Green Chem. **2013**, 15, 2929-2934.
- [15] K. Chen, K. Mori, H. Watanabe, Y. Nakagawa, K. Tomishige, J. Catal. **2012**, 294, 171-183.
- [16] S. Liu, Y. Amada, M. Tamura, Y. Nakagawa, K. Tomishige, Green Chem. **2014**, 16, 617-626.

Formatat: angles (EUA)

- [17] a) S. Koso, N. Ueda, Y. Shinmi, K. Okumura, T. Kizuka, K. Tomishige, *J. Catal.* **2009**, 267, 89–92. b) S. Koso, H. Watanabe, K. Okumura, Y. Nakagawa, K. Tomishige, *Appl. Catal., B* **2012**, 111–112, 27–37.
- [18] F. B. Gebretsadik, J. Ruiz-Martinez, P. Salagre, Y. Cesteros, *Appl. Catal., A*, DOI: 10.1016/j.apcata.2017.03.018.
- [19] F. B. Gebretsadik, D. Mance, M. Baldus, P. Salagre, Y. Cesteros, *Appl. Clay Sci.* **2015**, 114, 20–30.
- [20] M. Bartók1, A. Fási, F. Notheisz, *J. Catal.* **1998**, 175, 40–47
- [21] R. Mokaya, W. Jones, S. Moreno, G. Poncelet, *Catal. Lett.* **1998**, 49, 87–94.

WILEY-VCH

---

## FULL PAPER

## Entry for the Table of Contents (layout 2)

Layout 1:

## FULL PAPER

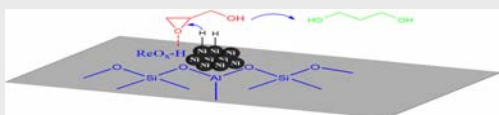
Text for Table of Contents

((Insert TOC Graphic here: max.  
width: 5.5 cm; max. height: 5.0 cm))

*Author(s), Corresponding Author(s)\****Page No. – Page No.****Title**

Layout 2:

## FULL PAPER

*Fiseha B. Gebrestadik,<sup>a</sup> Jordi Llorca,<sup>b</sup>  
Pilar Salagre,<sup>\*a</sup> Yolanda Cesteros<sup>a</sup>***Page No. 1– Page No. 12*****Hydrogenolysis of glycidol as  
alternative route to obtain selectively  
1,3-propanediol using MO<sub>x</sub> modified  
Ni-Cu catalysts supported on acid  
mesoporous saponite***